ELSEVIER

Journal of Power Sources 101 (2001) 167–176

JOURNAL OF POWER SOURCES

www.elsevier.com/locate/jpowsour

Analysis of ferrate(VI) compounds and super-iron Fe(VI) battery cathodes: FTIR, ICP, titrimetric, XRD, UV/VIS, and electrochemical characterization

Stuart Licht*, Vera Naschitz, Leonid Halperin, Nadezhda Halperin, Lin Lin, Jianjun Chen, Susanta Ghosh, Bing Liu

Department of Chemistry and Institute of Catalysis, Technion Israel Institute of Technology, Haifa 32000, Israel

Received 15 January 2001; accepted 21 January 2001

Abstract

Chemical and electrochemical techniques are presented for the analysis of Fe(VI) compounds used in super-iron electrochemical storage cells. Fe(VI) analytical methodologies summarized are FTIR, ICP, titrimetric, UV/VIS, XRD Fe(VI), potentiometric, galvanostatic, cyclic voltammetry, and constant load, current or power electrochemical discharges probes. The investigated FTIR methodology becomes quantitative with introduction of an internal standard such as added barium sulfate. Electrochemical techniques which utilize a solid cathode, and spectroscopic techniques which utilize a solid sample, are preferred over solution phase techniques. The titrimetric methodology (chromite analysis) has been detailed, and adjusted to determine the extent of Fe(VI → III) oxidation power in both unmodified or coated Fe(VI) compounds. Fe(VI) compounds have also been variously referred to as ferrates or super-iron compounds, and include K_2FeO_4 and $BaFeO_4$. Such compounds are highly oxidizing, and in the aqueous phase the full three electron cathodic charge capacity has been realized, as summarized by reactions such as: $FeO_4^{2-} + 5/2H_2O + 3e^- \rightarrow 1/2Fe_2O_3 + 5OH^-$.

Keywords: Ferrate analysis; Fe(VI) analysis; Fe(VI) cathode; Super-iron analysis; Super-iron battery; Alkaline battery

1. Introduction

Recently we presented the chemical preparation of high purity Fe(VI) salts for electrochemical storage. Synthetic pathways yielding 80–100 g of 96.5–99.5% pure K_2FeO_4 and $BaFeO_4$ were described, and the products of these syntheses were demonstrated to provide a high energy electrochemical discharge in a variety of cells [1]. The related analysis of Fe(VI) salts had not been detailed for the new field of Fe(VI) batteries. This associated paper summarizes approaches towards the direct chemical analysis of Fe(VI) compounds, and also their analysis when utilized as cathodes in super-iron batteries. Alkaline primary, metal hydride rechargeable, and lithium non aqueous examples of super-iron batteries utilizing Fe(VI) salts have been presented with several energy and environmental advantages [2–6]. Fe(VI) salts have a high oxidizing power, and in the aqueous phase the full 406 mAh g^{-1} K_2FeO_4 three electron cathodic charge capacity has been realized, as summarized by

$$FeO_4^{2-} + \tfrac{5}{2}H_2O + 3e^- \rightarrow \tfrac{1}{2}Fe_2O_3 + 5HO^- \quad (1)$$

Iron typically occurs as a metal, or in the valence states Fe(II) or Fe(III). Fe(VI) species have been known for over a century, although its chemistry remains relatively unexplored [7]. The term ''ferrate'' has been variously applied to both Fe(II) and Fe(III) compounds. Instead, due to their highly oxidized iron basis, multiple electron transfers, and high intrinsic energy, we refer to cells containing iron compounds in a greater than three valence state as ''super-iron'' batteries. The charge insertion or reduction of Fe(VI) represents an energetic and high capacity source of cathodic charge, and have been prepared as an environmentally benign (due to the ferric oxide product) cathode. Fe(VI) salts have been prepared from readily available ferric salts, such as in

$$Fe(OH)_3 + \tfrac{3}{2}ClO^- + 2OH^- \rightarrow FeO_4^{2-} + \tfrac{2}{3}Cl + \tfrac{5}{2}H_2O \quad (2)$$

* Corresponding author. Tel.: +972-4-8292963; fax: +972-4-8293015.
E-mail address: chrlicht@techunix.technion.ac.il (S. Licht).

0378-7753/01/$ – see front matter
PII: S0378-7753(01)00786-8

This study focuses on chemical and electrochemical techniques for the analysis of Fe(VI) compounds used in super-iron electrochemical storage cells. Analytical Fe(VI) methodologies which are investigated and summarized are FTIR, ICP, titrimetric (chromite), UV/VIS, XRD Fe(VI), potentiometric, galvanostatic, cyclic voltammetry, and constant load, current or power electrochemical discharges.

2. FTIR Fe(VI) analysis

The use of FTIR as a quantitative tool for the determination of Fe(VI) compounds is developed and demonstrated in this section. We have found a suitable Fe(VI) FTIR standard, to be added as a constant fraction to an Fe(VI) sample mix with the favorable characteristics: (i) that is inert towards Fe(VI) compounds; and (ii) with a clear, intrinsic IR spectra isolated from the Fe(VI) absorption bands. Fig. 1 presents the transmittance FTIR spectra of K_2FeO_4 and $BaFeO_4$, as measured in a conventional KBr pellet. The spectra are presented after baseline correction, using as a blank the same KBr pellet but in the absence of Fe(VI). As can be seen, the spectra are readily distinguishable, and are consistent with the previous IR and FTIR qualitative determination of several Fe(VI) compounds [8,9]. The small sample size, comprising 0.1 to 1% by weight of the KBr pellet, as well as the precise placement of the pellet in the spectrometer, provides challenges to the quantitative analysis of the spectra. These challenges are overcome by the use of an added standard, added as a fixed concentration to the sample, prior to extracting a segment of the sample to prepare the KBr pellet.

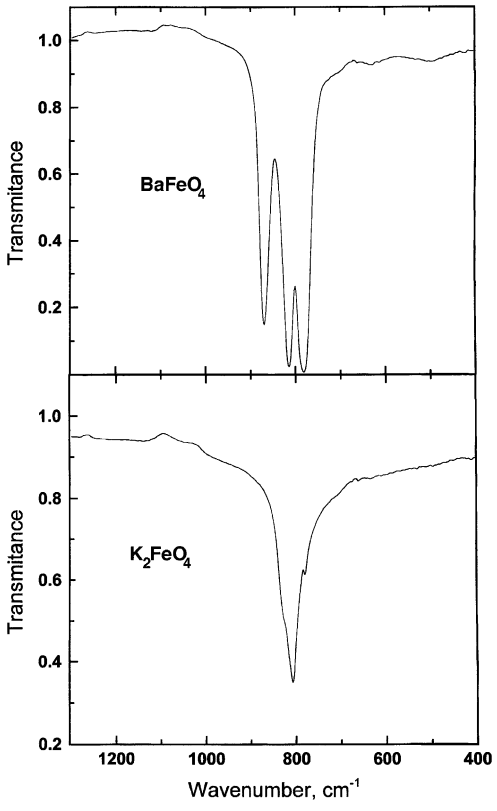

Fig. 1. Transmittance FTIR of BaFeO4 (top) and K_2FeO_4 (bottom).

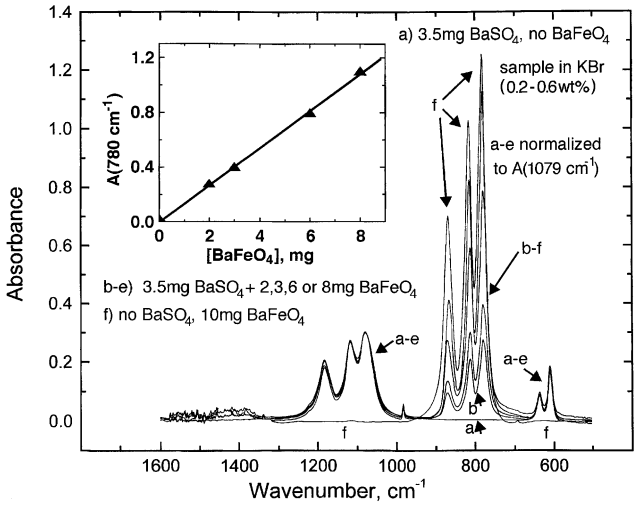

Fig. 2. Absorbance FTIR analysis of $BaFeO_4$ utilizing a $BaSO_4$ standard.

The Fe(VI) standard is provided by addition of barium sulfate and provides reproducible, inert, and distinctive, but isolated, IR absorption. As seen in Fig. 2 and in the figure insert, the absorbance of $BaFeO_4$ at 780 cm^{-1}, relative to the $BaSO_4$ absorbance at 1079 or 1183 cm^{-1}, of a fixed concentration or $BaSO_4$, grows in linear proportion to the $BaFeO_4$ concentration, and provides a route for quantitative analysis of the $BaFeO_4$ concentration. The analysis utilizes κ, the $BaSO_4$ to $BaFeO_4$ conversion constant, defined by the absorptivity of $BaSO_4$ compared to that of $BaFeO_4$, in a standard sample containing equal $BaSO_4$ and $BaFeO_4$ weight fractions.

$$\kappa\,(\text{wt.\%}\,\text{BaFeO}_4 = \text{wt.\%}\,\text{BaSO}_4) \equiv \frac{A_{\text{BaSO}_4}(1079\,\text{cm}^{-1})}{A_{\text{BaFeO}_4}(780\,\text{cm}^{-1})} \tag{3}$$

From the magnitude of the absorption spectra in Fig. 2 an appropriate methodology for FTIR analysis of an unknown in $BaFeO_4$ is suggested: (i) prepare a 100 mg of sample comprising two parts of the unknown with one part by weight of $BaSO_4$; thereby forming a sample with a constant fraction $f = 1/3$ in $BaSO_4$; (ii) prepare a KBr pellet containing ~1 wt.% of this admixture; (iii) measure and baseline correct the FTIR spectrum; (iv) calculate the relative $BaFeO_4$ to $BaSO_4$ absorption peaks, as R from the measured absorption peaks

$$R = \frac{A(780\,\text{cm}^{-1})}{A(1079)} \tag{4}$$

which determines the $BaFeO_4$ concentration in the $BaSO_4$ sample admixture

$$[BaFeO_4, \text{wt.}\% \text{ in } BaSO_4 \text{ admixture}] = 100\% R\kappa f \quad (5)$$

(v) convert this ratio, by $f/(1-f)$, to the composition of $BaFeO_4$ in the unknown as

$$BaFeO_4, \text{wt.}\% \text{ determind in unknown}] = 100\% \frac{R\kappa}{f^{-1}-1} \quad (6)$$

where κ is the $BaSO_4$ to $BaFeO_4$ conversion constant may be determined from a mixture containing equal weight fractions of $BaSO_4$ and $BaFeO_4$ and measured as $1/R$. More precisely, κ, may be determined using the inverse slope of a calibration curve of $[BaFeO_4]/[BaSO_4]$ versus R measured in $f = 1/3$ $BaSO_4$ mixes, with KBr and also containing 0, 4, 10, 20, 33, 50, or 66 wt.% known, pure $BaFeO_4$ (e.g. 100 mg samples containing 33.3 mg $BaSO_4$, and either, 0, 4, 10, 20, 33.3, 50 or 66.7 mg $BaFeO_4$, with the remainder as added KBr). Calibration of κ, will compensate for path length, spectrometer, $BaSO_4$ and Fe(VI) material composition variations (for example, a sample which contains additional Fe(VI) salts or other interferences). However, in the absence of a pure $BaFeO_4$ sample, a $\kappa = 1.15$ is appropriate.

The quantitative Fe(VI) analysis capability can be of significance when FTIR will be used as a tool to probe the extent of discharge, and the discharge products for Fe(VI) cathodes. This is exemplified in initial results (utilizing a 1:1, rather than the recommended 1:2, admixture of $BaSO_4$) presented in Fig. 3 and summarizing the FTIR spectra of an $BaFeO_4$ cathode at various stages of battery discharge. The Fe(VI) cathode mix is removed from an alkaline super-iron (AAA Zn anode) battery, the $BaSO_4$ standard is added, and the cathode mix is analyzed intact (without washing or removal of the graphite or electrolyte from the cathode mix) to reveal information regarding the Fe(VI) electrochemical discharge products. The $BaFeO_4$ absorption peaks are observed to fall at higher depth of discharge. With discharge, a peak is observed to grow at 1436 cm^{-1}, as well as smaller peaks at 857 and 692 cm^{-1}. The location and magnitude of these peaks correlate with the FTIR absorption spectra we observe for pure $Ba(OH)_2 \cdot 8H_2O$, and differ from the spectra we measure for Fe_3O_4 or Fe_2O_3 or the known IR spectra of simple, lower valence state Fe salts [9–11].

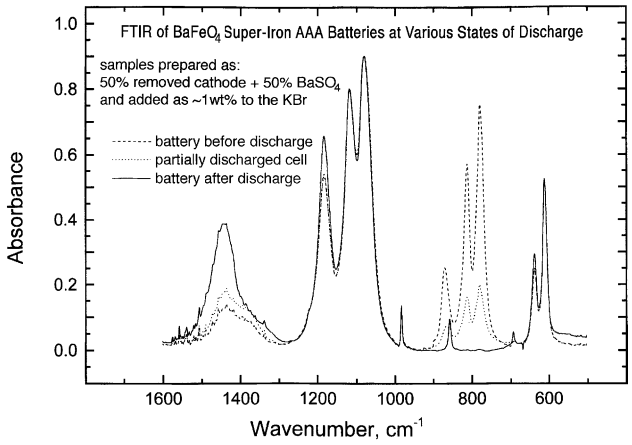

Fig. 3. Absorbance FTIR analysis of the Fe(VI) cathode mixture removed at various levels of cell discharge from ($BaFeO_4$) super-iron alkaline (Zn anode) AAA cells.

3. ICP Fe(VI) analysis

Inductively coupled plasma analysis of K_2FeO_4 and $BaFeO_4$ samples was conducted with a ICP Perkin-Elmer Optima 3000 DV to determine the relative weight percent and mole percent compositions of the principal cations, and possible impurities, in the sample. Such conventional inductively coupled plasma analytical methodologies provide elemental composition information, but not information regarding a compound's valence state. Hence, these methodologies are convenient, but not specific, to Fe(VI) analysis, and are only briefly described in this study. These methodologies, or related atomic absorption or emission and X-ray fluorescence techniques, are important to determine total iron relative to other elements in a super-iron compound. From these values, the mole ratio of principal cations, the mass percent of the principal cations, and the maximum contribution of alternate cation impurities is determined. Examples of ICP results are summarized in Table 1 for two salts K_2FeO_4 and $BaFeO_4$, which were subsequently determined to contain over 98% of the Fe as

Table 1
Inductively coupled plasma determined elemental constituents measured in high purity K_2FeO_4 and $BaFeO_4$ samples[a]

Sample	Mass (mg)	Fe by mass (%)	K by mass (%)	Ba by mass (%)	Sr by mass (%)	Na by mass (%)	Li by mass (%)
K_2FeO_4	35.8	28.2	39.4	<0.05	<0.05	<0.08	<0.05
$BaFeO_4$	49.0	21.5	0.2	53.0	0.6	<0.08	<0.05
		Mole ratio of main cation: Fe		ICP moles Fe, relative to mass equivalents Fe (%)		Chromite Fe(VI), relative to mass equivalents Fe (%)	
K_2FeO_4		2.003		99.3		98.6	
$BaFeO_4$		0.997		99.0		98.1	

[a] From these mass constituents are determined the mole ratio of principal cations and the Fe relative to the structural Fe. For comparison purposes, the Fe(VI) determined by chromite analysis is also included in the table. The indicated sample mass, normalized by the K_2FeO_4 or $BaFeO_4$ formula weight, yields the (theoretical) mass equivalents of iron used in the determination of relative ICP moles Fe or chromite Fe(VI).

Fe(VI) by chromite analysis according to the procedure described in the subsequent section. Note in Table 1 a main impurity (at 0.6% impurity levels) is strontium in the $BaFeO_4$ samples. The strontium is a component of the (otherwise analytical reagent) $Ba(OH)_2$ used in the $BaFeO_4$ synthesis.

4. Titrimetric (chromite) Fe(VI) analysis

4.1. Overview of Fe(VI) chromite analysis

Following the quantitative determination of total iron in a compound, for example, as described by ICP analysis in the previous section, the extent of the iron existing in the Fe(VI) valence state can be determined by titrimetric chromite analysis. Alternately, if the type of Fe(VI) compound is known (for example, as K_2FeO_4 or $BaFeO_4$), then the sample's mass yields the theoretical oxidation capacity (calculated as three equivalents per Fe), which in turn is compared with the chromite analyzed oxidation capacity.

The chromite analysis methodology varies with the specific Fe(VI) compound to be ascertained, and was developed to probe high valence state iron [12]. For example, the highly insoluble $BaFeO_4$ compound must be heated during dissolution, and alternate competing oxidants must be removed. In this section are presented our optimized chromite methodologies for several Fe(VI) related materials. In each case, the Fe(VI) sample is dissolved into solution as FeO_4^{2-} to oxidize chromite, Cr(III) to chromate Cr(VI).

$$Cr(OH)_{4^-} + FeO_4^{2-} + 3H_2O \rightarrow Fe(OH)_3(H_2O)_3 + CrO_4^{2-} + OH^- \quad (7)$$

The generated chromate is then titrated with a standard ferrous ammonium sulfate solution, using a (0.5 g per 100 ml) aqueous sodium diphenylamine sulfonate indicator solution. Each of the examples of Fe(VI) chromite analysis methodologies described below utilizes analytical reagents in doubly deionized water.

The chromite analysis can be used to determined the stability of Fe(VI) compounds, when the oxidizing capacity of samples is measured over time, and compared to the (three electron) equivalents of Fe(VI → III) within the compound. Both K_2FeO_4 and $BaFeO_4$ are highly stable. Carefully prepared, chemically synthesized K_2FeO_4, is particularly robust, and the long-term stability (of over 1 year) of K_2FeO_4, as analyzed by chromite, is presented in Fig. 4.

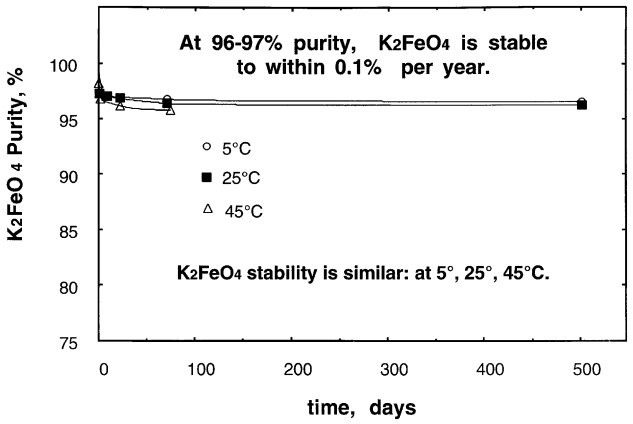

Fig. 4. Demonstration of the long term stability of K_2FeO_4, as determined by chromite analysis.

4.2. K_2FeO_4 chromite analysis

- Insertion of the solid K_2FeO_4 sample into solution

  A concentrated NaOH solution is prepared from 720 g NaOH in 1 liter of solution, and pretreated to remove potential interferences by reaction (boiling) with 0.1 g K_2FeO_4 until the characteristic purple/black FeO_4^{2-} color disappears. A Cr(III) solution is prepared from 16.66 g $CrCl_3 \times 6H_2O$ per 100 ml solution. A 20 ml of the pretreated, concentrated NaOH solution is combined with 5 ml of the Cr(III) solution, a further 5 ml of water is added, and the solution is cooled to room temperature in an ice bath. A 150–200 mg K_2FeO_4 sample is added to this solution, which is stirred for 30 min, until full K_2FeO_4 dissolution.
- Preparation of the solution to be titrated

  Prior to titration, to the K_2FeO_4 solution (or 25 ml of a known Cr(VI) solution) sequentially is added: 150 ml water, followed by 65 ml of $1/5H_2SO_4$ (prepared from a 1/5 dilution of 95–97% H_2SO_4), then 15 ml of a H_2SO_4/H_3PO_4 solution (prepared from 240 ml water, 150 ml 85% H_3PO_4, and 60 ml 95–97% H_2SO_4), and seven to eight drops of the sodium diphenylamine sulfonate indicator solution.
- Preparation of the 0.085 N ferrous ammonium sulfate titrant

  A 250 ml solution is prepared with 8.34 g $Fe(NH_4)_2(SO_4)_2 \times 6H_2O$. The precise normality of the ferrous ammonium sulfate solution is determined by using this solution to titrate a Cr(VI) known sample solution. The Cr(VI) solution is prepared from 25 ml of 0.085*N* $K_2Cr_2O_7$ solution (prepared as 1.042 g $K_2Cr_2O_7$ per 250 ml solution), and is treated as described above prior to titration. From the concentration of the K_2Cr_2O solution, the normality, *N*, of the ferrous ammonium sulfate is then determined from *V* (ml), the volume of $Fe(NH_4)_2(SO_4)_2 \times 6H_2O$ titrant needed to yield a color change from purple to green, as $N = 0.085 \times 25/V$.
- Determination of the K_2FeO_4 purity

  The K_2FeO_4 is inserted into solution and the solution prepared for titration as described above. From *V* (ml), the volume of $Fe(NH_4)_2(SO_4)_2 \times 6H_2O$ titrant needed in the titration to a color change from purple to green,

and the normality, N, of the ferrous ammonium sulfate, is then determined the K_2FeO_4 purity, $P(\%)$, as

$$P(\%) = \frac{100VN\,\mathrm{FW}}{3\,\mathrm{m}} \quad (8)$$

using the $\mathrm{FW} = 198.04\ \mathrm{g\ mol^{-1}}$ formula weight of K_2FeO_4, $n = 3$ equivalents per Fe(VI), and the sample mass m (mg).

4.3. Uncoated $BaFeO_4$ chromite analysis

- Insertion of the solid $BaFeO_4$ sample into solution, and preparation of the solution to be titrated

  As with the K_2FeO_4 sample, a concentrated NaOH solution is prepared from 720 g NaOH in 1 liter of solution, and pretreated by boiling with 0.1 g K_2FeO until the solution color disappears. A Cr(III) solution is again prepared from 16.66 g $CrCl_3 \times 6H_2O$ per 100 ml solution. Now however, 20 ml of the pretreated, concentrated NaOH solution is combined with 3 ml of the Cr(III) solution, and the solution is cooled to room temperature in an ice bath. A 100–110 mg $BaFeO_4$ sample is added to this solution, which is stirred for 30 min. Following addition of 50 ml distilled water, the mixture is heated to 90–95°C (using a water bath) for 1 h. After cooling, to the solution is added a cooled mixture of 240 ml water, 150 ml 85% H_3PO_4, 60 ml 95–97% H_2SO_4, and seven to eight drops of sodium diphenylamine sulfonate.
- Determination of the $BaFeO_4$ purity

  The $BaFeO_4$, inserted into solution and prepared for titration, is titrated with a ferrous ammonium sulfate solution prepared and standardized as described in the previous K_2FeO_4 chromite analysis section. From V (ml), the volume of $Fe(NH_4)_2(SO_4)_2 \times 6H_2O$ titrant needed to yield a color change from purple to green, and the normality, N, of the ferrous ammonium sulfate, is then determined from Eq. (8) using the 257.11 g $\mathrm{mol^{-1}}$ formula weight of $BaFeO_4$, and the sample mass m (mg).

4.4. Coated Ba_2FeO_4 chromite analysis

Low levels of coatings, such as 1–10% by weight $KMnO_4$, over Fe(VI) compounds have been shown to have an activating effect on these materials when discharged as a battery material. This alternate method increases the precision of chromite analysis for coated materials, and also provides a verification of the degree of coating, but requires substantially more material for analysis. First the coating is removed, without effecting the Fe(VI) valence state, and then analyzed by chromite. The method utilizes sonification in acetonitrile to remove the coating. $KMnO_4$ is soluble, but $BaFeO_4$ (or K_2FeO_4) is insoluble in acetonitrile. The acetonitrile solutions are then UV/VIS analyzed for $KMnO_4$. The sonification does not effect the purity, but it does diminish the average particle size, and significant amounts of material are subsequently lost during filtration from the acetonitrile.

To 1 g coated $BaFeO_4$ is added 75 ml dry acetonitrile which is then sonicated in an ultrasonic bath (operating amplitude 53 kHz) for 1 h at room temperature. The resultant suspension had a homogeneous dark red color. The suspension is filtered on a sintered glass filter, and the precipitate washed with 25 ml acetonitrile on the filter, and again sonicated in 75 ml acetonitrile for a second hour. The suspension is again filtered on a sintered glass filter, and the precipitate washed with 25 ml acetonitrile on the filter, and again sonicated in 75 ml acetonitrile for a third hour. The precipitate is once again filtered on a sintered glass filter, and washed with 25 ml acetonitrile on the filter. The precipitate is dried in vacuum for 18 h. The dried sample is weighed, and generally retains ~80% of its original mass, and the procedure generally removes >99% of a $KMnO_4$ coating. The Fe(VI) purity is subsequently determined as described in the prior sections.

5. UV/VIS Fe(VI) analysis

Fe(VI), dissolved as FeO_4^{2-}, has a distinctive UV/VIS spectrum. However, the quantitative analysis of solid Fe(VI) salts by dissolution and UV/VIS absorption spectroscopy is limited by (i) the relative insolubility of Fe(VI) salts such as $BaFeO_4$ in aqueous solutions [3], the general tendency of Fe(VI) salt insolubility in a wide variety of organic solvents [6] and the tendency of dissolved aqueous Fe(VI) salts to decompose in aqueous solutions other than specific electrolytes, such as highly concentrated KOH electrolytes; and (ii) electrolytes specifically excluding Ni(II) and Co(II) catalysts [2]. The decomposition with water takes the form of

$$2FeO_4^{2-} + 3H_2O \rightarrow 2FeOOH + \tfrac{3}{2}O_2 + 4OH^- \quad (9)$$

When occurring, the decomposition tends to lead to the formation of colloidal ferric(III) oxide, and to limit the time available for Fe(VI) analysis. Colloidal ferric oxide interference is minimized by a 385 nm baseline correction, and/or solution centrifugation prior to spectroscopic analysis. The visible absorption spectrum of ferrate(VI) in highly alkaline solution is presented in the inset of Fig. 5. This shows a maximum at 505 nm, an absorption shoulder at 570 nm and two minima at 390 and 675 nm. The molar absorptivity measured at 505 nm is $1070 \pm 30\ \mathrm{M^{-1}\ cm^{-1}}$. The molar absorptivity remained constant up to 200 mM. Similarly, at a fixed ferrate concentration, the measured absorbance was independent of alkali hydroxide cation and concentration. Hence, to within better than 5%, the 505 nm absorbance of 2 mM K_2FeO_4 is the same in 5 M lithium, sodium, potassium and sodium hydroxide, and also the same in 5–15 M NaOH, 5–13.5 M KOH and 5–15 M CsOH.

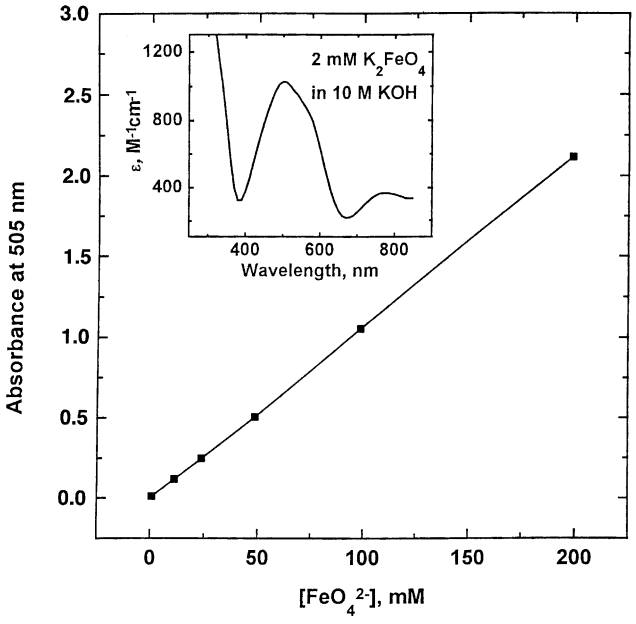

Fig. 5. The 505 nm absorbance of ferrate(VI) solutions of various concentrations at 505 nm. Inset: VIS absorption spectra of FeO_4^{2-} in aqueous solutions.

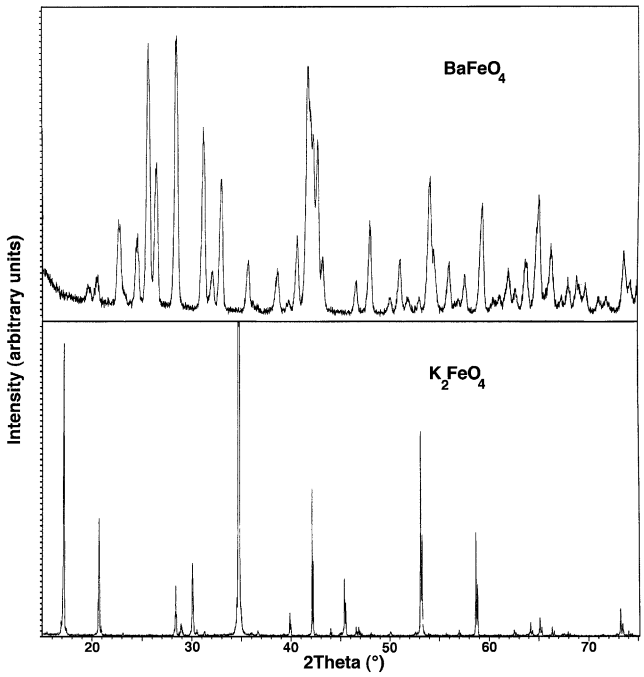

Fig. 6. Powder X-ray diffraction measurement of $BaFeO_4$ (top) and K_2FeO_4 (bottom).

The catalytic acceleration of Fe(VI) decomposition in solution is evident with less than 1 μM Ni(II). At the lowest Ni(II) concentrations, solution pre-treatment (such as inducing decomposition of 2 mM K_2FeO_4 in KOH solution at 60–80°C, followed by removal of the decomposition products) can improve the subsequent Fe(VI) stability. The solubility of Fe(VI) salts is low in this solution [2–4], but the stability of the dissolved FeO_4^{2-} is high [2]. A useful procedure for UV/VIS analysis of a solid Fe(VI) sample is to first prepare a solution of this pre-treated saturated KOH. Attempt to dissolve a precise mass (2–3 mg) of the sample in 10 ml (∼1 mM Fe(VI)) of the pre-treated saturated KOH solution. Measure the UV/VIS spectrum, and baseline correct to avoid 385 nm colloidal ferric oxide interference. Determine the absorbance at 505 nm and convert to FeO_4^{2-} concentration. Note, that the presence of $Ba(OH)_2$ will further diminish FeO_4^{2-} solubility. This increases the challenge to dissolve a solid Fe(VI) sample. $BaFeO_4$ is insoluble in aqueous saturated $Ba(OH)_2$. In KOH solutions also containing saturated $Ba(OH)_2$, $BaFeO_4$ dissolves only at the submillimolar level [3].

6. XRD Fe(VI) analysis

We have measured Fe(VI) powder XRD data using a Philips analytical X-ray, BV diffractometer, operating with Cu Kα radiation, with a flat sample holder mounted on a SPG spectrogoniometer. Representative powder X-ray diffraction spectra of K_2FeO_4 and $BaFeO_4$ are presented in Fig. 6 and exhibit little variation using salts ranging averaging in particle size from 35 to 100 μm, or measured with a wide range of (2θ) scan rates. The obtained XRD spectra of both K_2FeO_4 and $BaFeO_4$ are in good agreement with the previously measured powder X-ray diffraction patterns by Herber and Johnson and others [13,14]. The spectra are consistent with an orthorhombic crystal system with the spaces group D_{2h} (Pnma) [13]. We observe that typical $BaFeO_4$ XRD patterns are less sharp than those observed for K_2FeO_4, under equivalent measurement conditions, and as summarized in Fig. 6. However, this may reflect our synthetic technique [1], rather than an intrinsic property of these salts.

Although often used as a tool for qualitative rather than quantitative, analysis, we also use XRD to distinguish between coated barium ferrate from pure barium ferrate. For example, a several percent coating from $KMnO_4$ is distinguishable as a low level of the expected, known $KMnO_4$ XRD pattern superimposed on the regular $BaFeO_4$ pattern. Graphites and carbon blacks added to an Fe(VI) mix in the preparation of a cathode do not significantly interfere with the observed Fe(VI) XRD patterns. We are attempting to distinguish the products of a Fe(VI) cathode at various stages of discharge. However, the generally observed amorphous nature of the discharge products provides a challenge to the analysis.

7. Electrochemical Fe(VI) analysis

7.1. Overview of Fe(VI) electrochemical analysis

Electroanalytical techniques to probe Fe(VI) compounds can be conveniently categorized as either solution phase

(dissolved Fe(VI)) or solid cathode techniques. Analogous to circumventing challenges associated with the UV/VIS analysis of dissolved Fe(VI) described in a previous section, the solid cathode electrochemical techniques preclude possible problems arising from solution phase decomposition of Fe(VI) (including limited time for the analysis and the build up of competing ferric oxides) which can be associated with solution phase electrochemical Fe(VI) analysis. Nevertheless, the solution electrochemical techniques such as potentiometric, galvanostatic and cyclic-voltammetry methods are convenient, and are included in this section. In each of the solution phase techniques, the electrochemical characterization was carried out using a AFCBP1 Pine bipotentiostat in a three-electrode electrochemical cell. The working and counter electrodes were made of bright platinum. The reference electrode was saturated calomel electrode (SCE).

The solid cathode methodologies are largely free of the challenges associated with the solution phase techniques, and provide a direct probe of the kinetic (as a function of fixed load, current or power densities) and thermodynamic (as a function of cell potential) oxidizing capacity of the Fe(VI) compounds. In the solid cathode methodologies, the various different discharge modes will be described, but generally the potential was measured in time via LabView data acquisition on a PC, and cumulative discharge, as ampere hours (Ah), and watt hours (Wh), determined by incremental integration.

7.2. Fe(VI) potentiometric analysis

The measured redox potentials, at platinum electrode, of 2, 20, 60 and 100 mM K_2FeO_4 in various NaOH solutions are presented in Table 2. As expected, redox potential shifts to more positive values with an increase in ferrate concentration. As seen in the table, the concentration of NaOH has an effect on the measured ferrate redox potential in solutions. The observed considerable deviation, from the Eq. (1) three electron Nernstian slope of 20 mV, is presumable related to the high ionic strength of the medium. From the values in Table 2, extrapolation to zero ferrate concentration, yields the following ferrate potentials in sodium hydroxide, V versus SHE:

$$\text{in 5 M NaOH} : E_{FeO_4^{2-}} = 0.668 + 0.034 \times \log([FeO_4^{2-}]) \quad (10)$$

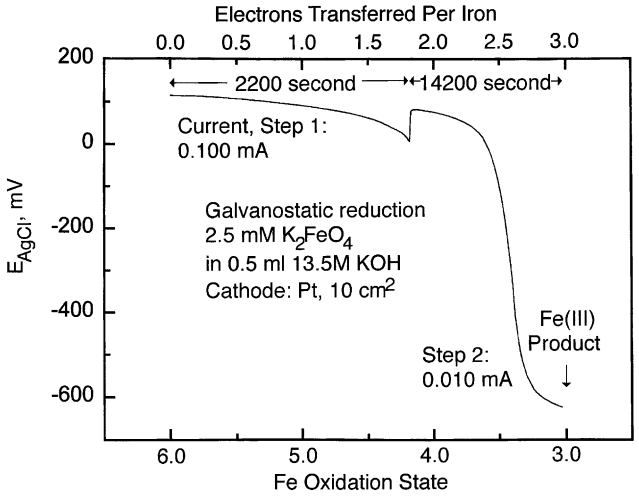

Fig. 7. Galvanostatic determination of the measurement of the oxidation state of iron in ferrate(VI) solutions.

$$\text{in 10 M NaOH} : E_{FeO_4^{2-}} = 0.661 + 0.040 \times \log([FeO_4^{2-}]) \quad (11)$$

$$\text{in 15 M NaOH} : E_{FeO_4^{2-}} = 0.661 + 0.043 \times \log([FeO_4^{2-}]) \quad (12)$$

$$\text{Yielding } E^{\circ}\,(\text{in NaOH})_{FeO_4^{2-}} = 0.66 \pm 0.01 \text{ V (SHE)}$$

In aqueous alkali and alkali earth hydroxide electrolytes, we have observed that a variety of Fe(VI) compounds, over a wide concentration range, exhibit a potential varying from 0.55 to 0.75 V versus SHE.

7.3. Fe(VI) solution phase galvanostatic analysis

Galvanostatic reduction of dissolved ferrate yields a direct electrochemical measurement of the oxidation state of iron in ferrate. Fig. 7 presents the time evolution of the potential, during ferrate reduction. A $c_{initial} = 2$ mM potassium ferrate solution in $v = 3$ ml of 15 **M** NaOH is reduced at a current density $J = 10\ \mu A\ cm^{-2}$. Integration of the charge transferred yields the relative oxidation state, $\Delta q'$, where F is the Faraday constant and t time.

$$\Delta q' = \frac{t \times J}{c_{initial} \times v \times F} \quad (13)$$

and which may be compared to the intrinsic charge of the insoluble Fe(III) product. A planar platinum electrode does

Table 2
Open circuit potential of Pt electrode in various alkaline ferrate, Fe(VI) solutions

[NaOH] (M)	Open circuit potential vs. SCE mV in solutions with various concentrations of K_2FeO_4			
	2 mM (mV)	20 mM (mV)	60 mM (mV)	100 mM (mV)
5	335	365	384	392
10	312	345	369	380
15	292	330	355	365

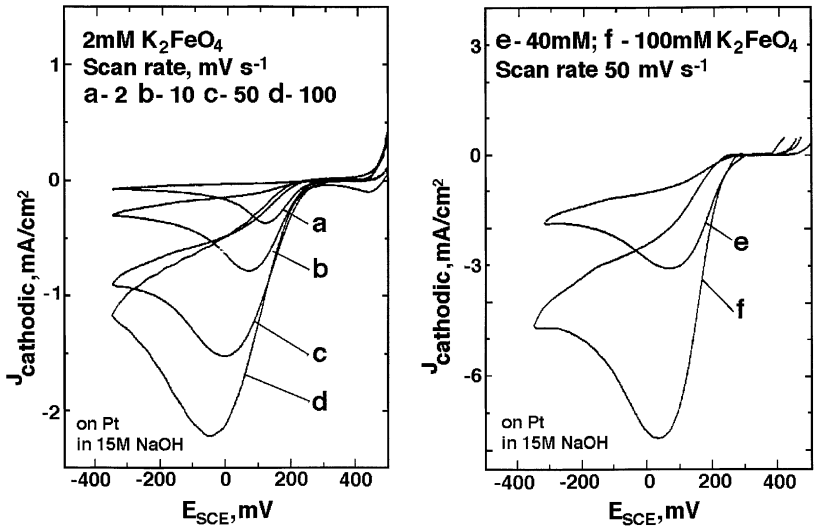

Fig. 8. Cyclic voltammetry of ferrate(VI) solutions. Left: variation with potential scan rate. Right: variation with ferrate(VI) concentration.

not provide the optimum surface to probe solution phase Fe(VI) reduction. The Pt surface tends to passivate in time as the reduced Fe(III) layer builds on the surface. This passivation is alleviated by (i) minimizing the thickness of the layer, employing low volumes and low concentrations of dissolved Fe(VI) salts; (ii) using low initial current densities, such as 10 μA cm^{-2}; and (iii) further diminishing the current by an order of magnitude as the overpotential increases towards the end of the reduction. Under these conditions, and as seen in the curve in Fig. 7, the oxidation state of the starting material approaches Fe(VI) in accord with Eq. (1).

7.4. Fe(VI) cyclic voltammetry analysis

Representative voltammetric curves for the reduction of K_2FeO_4 dissolved in 15 M NaOH at a Pt electrode are shown in Fig. 8. The negative potential scan reveals a cathodic current of ferrate(VI) reduction at potentials less positive than 200 mV. Thus, cathodic reduction of ferrate(VI) proceeds with an overvoltage of ~150 mV. Oxygen evolution in the oxidation sweep interferes with oxidation of ferrate(III). The peak cathodic current density increased linearly with ferrate concentration and was proportional to square root of the scan rate, indicating diffusion limitation of ferrate(VI) reduction. Measurements in solutions of electrochemically prepared ferrate(VI), rather than chemically synthesized FeO_4^{2-}, generate identical cyclic voltammograms.

7.5. Fe(VI) solid cathode discharge analysis

Using a cathode mixed with a high level of (30% by weight) of an effective conductive matrix (1 μm graphite [4]), the full 406 mAh g^{-1} storage capacity of K_2FeO_4 is obtained during discharge (as seen in Fig. 9) and in accord with the Fe(VI → III) $3e^-$ reduction, for example, as described in Eq. (1). The observed K_2FeO_4 cathodic charge capacity is 32% greater than the equivalent MnO_2. As exemplified by the history of MnO_2 optimization, and as seen for Fe(VI), coulombic efficiency will be further affected by other additives than graphite, and control of packing, electrolyte and particle size [2–6]. The average discharge potential of the K_2FeO_4 cathode of 1.58 V versus zinc, is 24% greater than the average for the equivalent manganese dioxide cell (1.27 V), both determined to 90% depth of discharge (Fig. 9). Combined with the increased charge capacity, this potential also leads to a further increase in comparative energy capacity.

Fig. 9 summarizes constant current discharge results obtained in a relatively small button configuration cell. Useful analytical information may also be obtained with larger cells packed with a Fe(VI) compound cathode mix, using cell configurations such as the conventional AAA dimensioned cylindrical cell, and again using a KOH electrolyte, and the remaining components removed from a commercial alkaline cell (including the Zn gel anode, the separators, the anode current collector, and the cathode current collector (the outer case)). Depending on the AAA cell configuration, such cell cells are packed with 1.1–1.4 Ah (3.5–4.5 g) of $BaFeO_4$, and discharged.

Fig. 10 presents discharge characteristics of three AAA $BaFeO_4$ alkaline cells, each prepared with an identical (1.3 Ah) $BaFeO_4$ cathode but discharged under the different high rate conditions of either a constant power of 0.7 W, a constant current of 0.5 A, or constant load of 2.8 Ω. The discharge curve is measured in time, and in the figure, respectively, plotted as either the total energy generated in Wh, or the charge storage capacity generated in the Ah, or as a percent of the intrinsic Fe(VI) capacity. The latter is determined by comparing the $3e^-$ equivalents in the measured charge capacity, to the theoretical capacity in the measured mass of the Fe(VI). Note, that the chosen

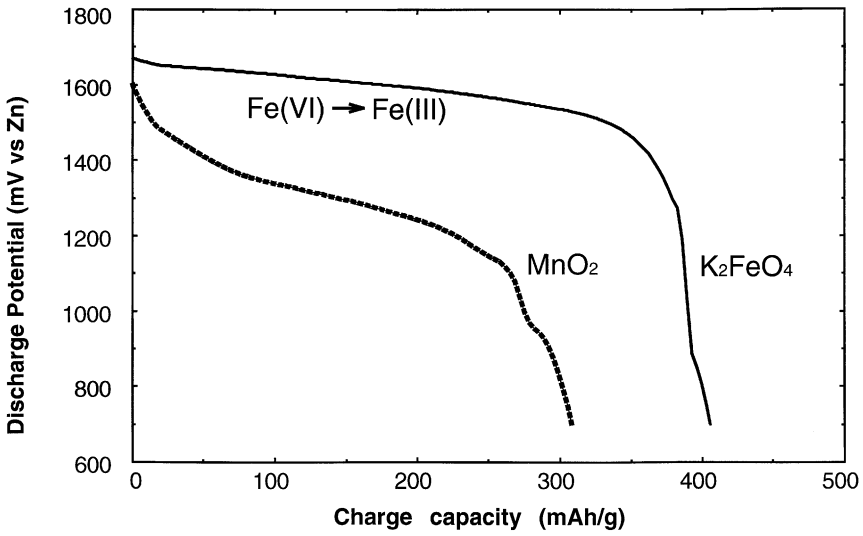

Fig. 9. Constant current (0.5 mA cm^{-2}) discharge of a K_2FeO_4 cathode compared to a MnO_2 cathode-limited Zn cell. Cell discharge is measured with Labview software interfaced pine model AFCBP1 bipotentiostat at 22°C. The cathode consists of either 17.3 mg (7 mAh) K_2FeO_4 or 22.7 mg (7 mAh) MnO_2, mixed with 30% graphite by weight. In each case, a commercial 1.1 cm diameter button cell, containing excess Zn, is opened, the cathode removed, and replaced with the 7 mAh cathode.

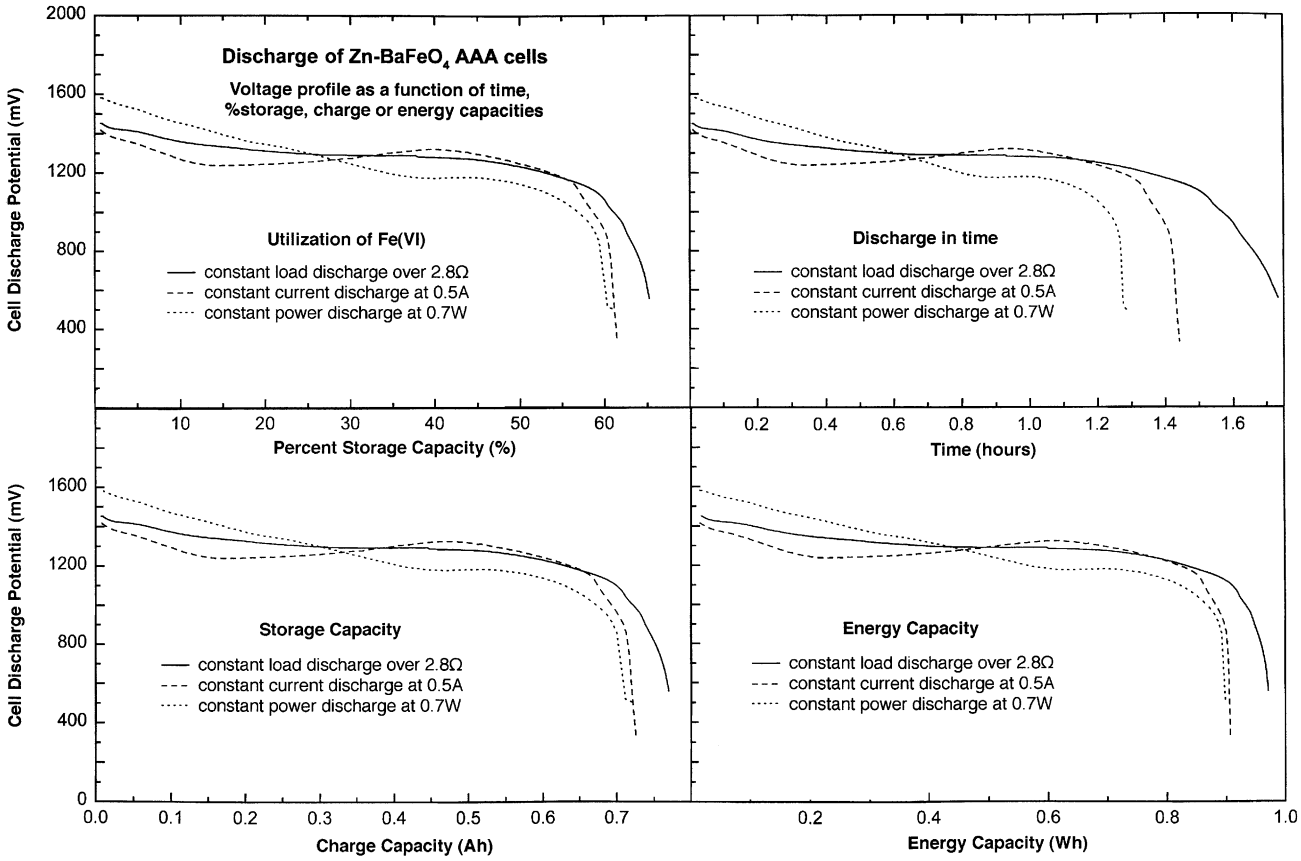

Fig. 10. Cell potential variation during discharge of alkaline barium super-iron AAA cells. Each cell contains a cathode mixed comprised of 4.16 g of 5% $KMnO_4$ coated $BaFeO_4$, 0.47 g 1 μm graphite, 0.047 g $Ba(OH)_2{\cdot}8H_2O$, and 0.55 g saturated KOH electrolyte. The cylindrical AAA cell configuration and experimental discharge conditions are further described in the text. The percent storage capacity is determined by the measured cumulative ampere hours, compared to the theoretical capacity.

high rate conditions of 0.7 W, 0.5 A, or 2.8 Ω, are similar, leading to similar discharge curves in the constant power, constant current or constant load discharge modes. These measured capacities are high compared to conventional alkaline cells [2], and can approach 100% of the theoretical Fe(VI) capacity at lower rate conditions [2–5].

8. Conclusions

Fe(VI) compounds have also been variously referred to as ferrates or super-iron compounds, and include K_2FeO_4 and $BaFeO_4$. Analytical Fe(VI) methodologies are investigated and summarized for the analysis of Fe(VI) compounds used in super-iron electrochemical storage cells. Such compounds are highly oxidizing, and in the aqueous phase the full three electron cathodic charge capacity has been realized.

Chemical and electrochemical analytical methodologies presented for the analysis of Fe(VI) compounds used in super-iron electrochemical storage cells include FTIR, titrimetric (chromite), UV/VIS, XRD Fe(VI), ICP, potentiometric, galvanostatic, cyclic voltammetry, and constant load, current or power electrochemical discharges. The FTIR methodology becomes quantitative with use of an internal standard such as added barium sulfate. Electrochemical techniques which utilize a solid cathode and spectroscopic techniques which utilize a solid sample are preferred over solution phase techniques. The chromite methodologies can be modified to determine the extent of Fe(VI → III) oxidation power in both unmodified or coated Fe(VI) compounds.

Acknowledgements

We thank N. Halperin, L. Halperin, J. Li, S. Shesternin and V. Nair, who participated in synthesis of the Fe(VI) compounds, and B. Wang, G. Levitin, and M. Greenberg, V. Goldstein, O. Khaselev, and E. Kvashnina who participated in the spectroscopic and/or electrochemical analyses.

References

[1] S. Licht, V. Naschitz, B. Liu, S. Ghosh, N. Halperin, L. Halperin, D. Rozen, J. Power Sources (2001), in press.
[2] S. Licht, B. Wang, S. Ghosh, Science 285 (1999) 1039.
[3] S. Licht, B. Wang, S. Ghosh, J. Li, V. Naschitz, Electrochem. Commun. 1 (1999) 522.
[4] S. Licht, B. Wang, G. Xu, J. Li, V. Naschitz, Electrochem. Commun. 1 (1999) 527.
[5] S. Licht, B. Wang, J. Li, S. Ghosh, R. Tel Vered, Electrochem. Commun. 2 (2000) 535.
[6] S. Licht, B. Wang, Electrochem. Solid State Lett. 3 (2000) 209.
[7] M.D. Johnson, J.F. Read, Inorg. Chem. 35 (1996) 6795.
[8] R.J. Audette, J.W. Quail, Inorg. Chem. 11 (1972) 1904.
[9] Y. Wang, A. Muramatsu, T. Sugimoto, Colloids Surf. 134 (1998) 281.
[10] A. Saric, S. Music, K. Nomura, S. Popvic, J. Mol. Struct. 481-1 (1999) 633.
[11] A.K. Tripathi, V.S. Kamble, N.M. Gupta, J. Catal. 187 (1999) 332.
[12] H. Goff, R.K. Murmann, J. Am. Chem. Soc. 93 (1971) 6058.
[13] R.H. Herber, D. Johnson, Inorg. Chem. 18 (1979) 2786.
[14] R.J. Audette, J.W. Quail, W.H. Black, B.E. Robertson, J. Solid State Chem. 8 (1973) 49.